Adaptive Control System for Biogas Power Plant Using Model Predictive Control

Samaa Fawzy, Mohammed Saeed, Abdelfattah Eladl, and Magdi El-Saadawi

***Abstract*—This paper presents an adaptive control system using model predictive control for a biogas-fueled power system. The control scheme is derived from an anaerobic digestion model that includes the concentration of biodegradable volatile solid in the reactor, the concentration of volatile solid in influent, the concentration of acidogens, and the concentration of methanogens. All these concentrations are the state variables of model predictive control. The whole biogas-fueled power system has been modeled, implemented, and tested in MATLAB/Simulink environment. To validate the performance of the proposed controller, different operation conditions are studied and analyzed. The simulation results prove the effectiveness and the applicability of the proposed control system under different operating conditions.**

***Index Terms*—Anaerobic digestion, micro-turbine, model predictive control, state space, biogas.**

I. Introduction

BIOGAS production from organic waste and/or energy crops has been continuously developing as a promising technology for heat and electricity production [1]. Anaerobic digestion (AD) includes a series of biological processes in which microorganisms break down biodegradable material in the absence of oxygen. The fed substrates in the AD process include many kinds of materials including wastewater, fertilizer, energy crops and the organic fraction of municipal solid waste. The output biogas is mainly composed of methane and carbon dioxide [1].

From the viewpoint of operation safety, AD is intrinsically a very unstable process in which the variations of input variables (hydraulic flow rate, influent organic load) may easily lead to the washout of the process, i. e., a state where the bacterial life disappears [2].

The use of advanced control and optimization algorithms for a biogas plant provides an attractive solution to ensure stable operation conditions and increase biogas production. The AD process is a compound, nonlinear and high-dimensional process. It involves four stages dependent on each other, and each stage requires a different set of optimal process parameters. The process is related to various anaerobe, biochemical and physical reactions which require a different set of optimal process variables to control the AD output and achieve substrate regulation.

The AD is a compound, nonlinear and high-dimensional process. It involves four stages dependent on each other and each stage requires a different set of optimal process parameters. The process is related to various anaerobe, biochemical and physical reactions which require a different set of optimal process variables to control the AD output and achieve substrate regulation. On the other hand, the transfer functions in the paper represent the microturbine model. The whole biogas-fueled power system is modeled, implemented, and tested in MATLAB/Simulink environment. The biogas-fueled power system is composed of three main parts: a biogas AD reactor, a micro-turbine (MT) coupled to a permanent magnet synchronous generator, and a storage system. Hence, the whole system is complex and nonlinear.

Numerous control systems have been designed and applied to control the operation of the AD reactor in a biogas-fueled power system. The functions of these control systems can be summed up in two actions: to regulate the produced methane flow for the required power production, and to keep the volatile fatty acids (VFA) concentration in the permissible limits. Reference [3] presents a critical overview of the available automatic control technologies implemented in AD processes at different scales. References [4] and [5] propose a temperature control system based on model predictive control (MPC) method for controlling a practical pilot AD bioreactor fed with dairy waste. The aforementioned references have focused on feedback control with on-off control, proportional integral (PI) control, and feedforward control for controlling the methane gas flow on both simulated and practical reactors. Reference [6] develops a proposed adaptive controller for an anaerobic digester considering the input constraints. Many assumptions have been considered for the proposed controller including the biomass and chemical oxygen demand concentrations, the model parameters and the limits of model parameters. Reference [7] presents a nonlinear MPC algorithm to optimally control the AD process in biogas plants, but the MPC algorithm has been applied to a reduced detailed model called the anaerobic digestion model No. 1 (ADM1). References [8] and [9] present a closed-loop substrate feed control for agricultural biogas plants. A multi-objective nonlinear MPC has been proposed to control the composition and amount of the substrate to optimize the economic feasibility of a biogas plant whilst ensuring process

Manuscript received: March 19, 2019; accepted: January 19, 2020. Date of CrossCheck: January 19, 2020. Date of online publication: July 30, 2021.

This article is distributed under the terms of the Creative Commons Attribution 4.0 International License (http://creativecommons.org/licenses/by/4.0/).

S. Fawzy (corresponding author), M. Saeed, A. Eladl, and M. El-Saadawi are with the Electrical Engineering Department, Mansoura University, Mansoura, Egypt (e-mail: samaa.fawzy92@gmail.com; mohammedsaid@mans.edu.eg; eladle7@mans.edu.eg; m_saadawi@mans.edu.eg).

DOI: 10.35833/MPCE.2019.000170

stability. A nonlinear predictive controller has been implemented to control a simulated ADM1 assuming that all states are available. Therefore, a state space is not used. Reference [10] applies a model-based adaptive linearizing controller and a fuzzy controller to control the alkaline volatile, and VAF within the prescribed limits to ensure stable process conditions and avoid accumulation of VFA. Six states of a real AD reactor fed with effluents from a wood processing plant have been estimated using an asymptotic observer. The asymptotic observer is an open-loop estimator and has no tuning parameters. Reference [11] develops a generic advanced process control system to optimize the performance of AD.

Reference [12] implements a predictive controller based on transfer functions adapted to the ADM1. In that model, the flow rates of the primary and secondary wastewater sludge are considered as the uncontrolled variables, whereas the biogas production rate and its methane content are considered as the controlled variables. The optimization criterion of the controller contains the square of the control error, while the control signal usage is not included. Reference [13] proposes a novel multi-objective control strategy based on controlling both the concentration of VFA in the effluent and the methane flow rate for an up-flow sludge bed-filter reactor. Finally, [14] introduces a survey over the last 40 years about feed control of AD processes for renewable energy production. It is concluded that although sophisticated controllers are existent, full-scale biogas plants still operate without a closed-loop feed control.

The main objective of this paper is to develop an adaptive control system to control the fed substrate to the reactor of a biogas power plant according to the connected load which can efficiently respond to any variations of the connected electrical load. The proposed control system depends on MPC method for controlling the biogas-fueled power system. An MPC-based algorithm is used to detect the control inputs that result in the best-predicted behavior of the system according to any changes.

This paper proposes an adaptive control system for the whole biogas power plant based on the flexible response of the biogas plant to any load changes. An MPC-based algorithm is used to detect the control inputs, which results in the best-predicted behavior of the system according to any changes. The MPC algorithm is based on state space models. The proposed controller is developed to control the fed substrate according to the predicted load and to handle the expected changes in electrical load through the speed of MT according to the amount of methane stored in the storage system.

The main contributions of this paper can briefly be summarized as follows:

1) An adaptive control system using MPC for a biogas power plant based on state space is proposed and simulated.

2) The control system depends on both MT parameters and the methane quantity stored in the storage tank.

3) The simulation results of the proposed controller prove its effectiveness and applicability to adapt the biogas power plant operation under different operating conditions.

4) The proposed control system decreases the duration and values of disturbances according to unbalanced loading conditions, and hence, it can protect the MT from damage.

The rest of the paper is organized as follows. Section II presents the proposed adaptive control system. Section III presents a procedure for solving the problem. Section IV presents mathematical modeling and simulation of the proposed control system. The simulation results and system validation are presented in Section V. Finally, the paper is concluded in Section VI.

II. Proposed Adaptive Control System Based on MPC

The MPC method has evolved significantly over the past two decades, which is realized by improving the performance indicators for some future control sequences by using predictions of the output signal based on the process model while satisfying a set of constraints. MPC can handle the constraints on the manipulated and controlled variables in a systematic manner. Meanwhile, it can handle multivariable control problems naturally. Although MPC has been successful in industries with slow processes, further researches are still required to solve the computation problems with fast operations [15].

MPC algorithm depends on an internal dynamic model of the process, a history of past control moves, and an optimization objective function over the receding prediction horizon to calculate the optimal control moves. MPC algorithm uses the moving horizon method, which calculates a range of horizontal control movements. Initial control movements are performed, while the remaining calculated movements are ignored [16]. The process is then repeated at subsequent sampling times. With the increase of computation speed of computers, MPC can be applied to fast operations rather than locking to slow operations.

A basic structure model of MPC method is illustrated by Fig. 1 [17]. The model is applied to predict future outputs of the plant based on past and current values and optimal proposed future control actions. These actions are computed by the optimizer with consideration of the constraints as well as the cost function, where the future trace error is considered.

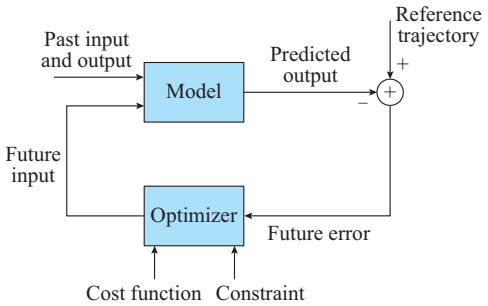

Fig. 1. Basic structure model of MPC.

The constraints can be either on the output of controlled processes (control variable) or on the control signals that are inputted to the process (manipulated variables). These constraints are in the form of saturation characteristics, for example, valves with a limited range of adjustment, a control surface with a limited deflection angle, etc. The input con-

straints are also shown in the form of rate constraints.

The MPC performance index is used to indicate how well the MPC controller is meeting its defined goal and how the model helps to achieve the better results. The index represents a measure for both the reference tracking error and the control action signal. The MPC performance index measures both the reference tracking error and the control action signal. The control law is established from the minimization of a two-norm measure of predicted performance. A typical performance index can be represented as [18]:

$$J=\sum_{i=n_w}^{n_y}\left\|R_{k+i}-Y_{k+i}\right\|+\lambda\sum_{i=0}^{n_u-1}\left\|U_{k+i}\right\| \tag{1}$$

where R_{k+i} is the reference signal at instant time k; Y_{k+i} is the weighted process output signal at instant time k; $\|\cdot\|$ is the norm operator; λ is the weight of the control action; U_{k+i} is the weighted process input signal at instant time k; n_w is the window parameter assumed to be one; n_y is the prediction horizon parameter; and n_u is the control horizon parameter.

In the MPC model, the receding horizon periods can be explained as follows.

1) At the k^{th} sampling instant, the values of the manipulated variables u are calculated at the next M sampling instants, $\{u(k), u(k+1), \ldots, u(k+M-1)\}$.

2) This set of M "control moves" is calculated so as to minimize the predicted deviations from the reference trajectory over the next P sampling instants while satisfying the constraints.

3) A linear program or quadratic program problem is solved at each sampling instant.

4) Set M as the control horizon and P as the prediction horizon.

5) Then, the first "control move", $u(k)$, is implemented.

6) At the next sampling instant, k+1, the M-step control policy is re-calculated for the next M sampling instants, $k+1$ to k+M, and the first control move $u(k+1)$ is implemented.

7) Then, 1) and 2) are repeated for subsequent sampling instants.

The prediction horizon is the design parameter of the MPC with an important effect on the computation cost of the controller. If a long prediction horizon is considered, the domain of attraction of the controller is larger and the performance is improved. However, the number of decision variables increases, and hence, the complexity of the optimization problem increases. The necessary condition for choosing the prediction horizon is the feasibility of the initial state. The model predictions can be written as [18]:

$$\hat{\boldsymbol{Y}}(k+1)=\boldsymbol{S}\Delta\boldsymbol{U}(k)+\hat{\boldsymbol{Y}}'(k+1) \tag{2}$$

where $\hat{\boldsymbol{Y}}(k+1)$ is the corrected prediction; $\hat{\boldsymbol{Y}}'(k+1)$ is the vector notation for predictions; $\Delta\boldsymbol{U}(k)$ is the k^{th} manipulated variable; and $\boldsymbol{S}$ is the dynamic matrix of dimension $P\times M$, M is control horizon, P is prediction horizon.

The control calculations are based on minimizing the predicted deviations between the reference trajectory. The predicted error is defined as [18]:

$$\hat{\boldsymbol{E}}(k+1)=\boldsymbol{Y}_r(k+1)-\hat{\boldsymbol{Y}}(k+1) \tag{3}$$

where $\hat{\boldsymbol{E}}(k+1)$ is the predicted error; and $\boldsymbol{Y}_r(k+1)$ is the reference trajectory.

This section presents a proposed control system for a biogas power plant using the MPC method. The MPC algorithms are based on state space models. The MPC algorithms represent a closed loop for controlling any variable signals in the biogas plant. MPC controls these signals and sends them to state space to predict the next state. It is important for the MPC to detect the current state of the biogas power plant. Therefore, the simulation begins with the current operation state of the biogas plant model. The MPC controller can be used to control the substrate feed and the amount of produced methane, as shown in Fig. 2.

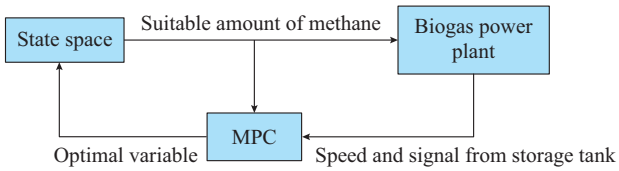

Fig. 2. Block diagram of proposed control system using MPC.

The optimal substrate feed can be achieved according to the current state of the plant depending on controlling the MT speed according to any load variations. The MT speed controller sends a signal to the MPC system to change the input feed amount based on the gas amount in the storage tank. Figure 3 shows a detailed schematic diagram of the proposed control system.

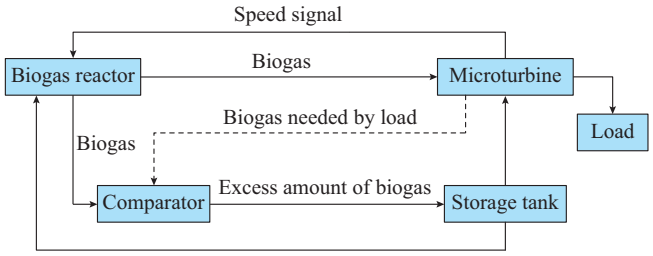

Fig. 3. Schematic diagram for proposed control system.

The methane formation in the reactor depends on the AD process (fermentation process), which takes a few days to produce a constant amount of the gas. Thus, the reactor must operate for a pre-operation period before connecting the electric load. After that period, the methane-fueled MT can be connected to the reactor, and the plant can supply electric loads. Three controllers are used to control the MT, i. e., a governor speed controller, a temperature controller, and an acceleration controller. The output of these controllers represents the input to a least value gate (LVG), whose output is the lowest value of the three inputs. The LVG sends a control signal which determines the least amount of fuel to the turbine, as illustrated in Fig. 4.

In case of increasing or decreasing the MT speed due to load change, the speed controller sends a signal to the MPC system to change the amount of feed input to the reactor based on the volume methane stored in the storage system. In this case, the amount of feed input to reactor change, and all the parameters of the AD process also change, including the concentration of biodegradable volatile solid in the reac-

tor, the concentration of volatile solid in influent, the concentration of acidogens, and the concentration of methanogens. This means that the system automatically changes its parameters according to the connected load.

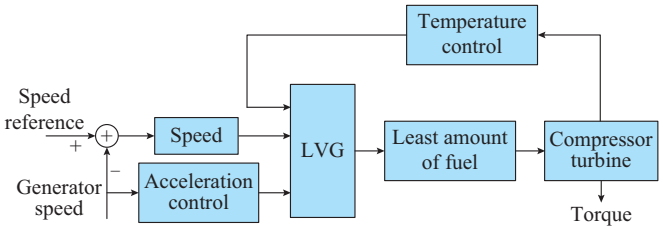

Fig. 4. Schematic diagram of an MT control function.

The MT is coupled to a high-speed generator directly driven by the turbo-compressor shaft to produce the required electric power. The fuel controller detects the suitable amount of methane to produce appropriate torque to drive a permanent magnet synchronous generator (PMSG) and supply the load. According to the methane requirements of MT, the MT sends a control signal to the comparator part of the storage system to compare it with the amount of methane produced by the reactor. If the produced methane is less than the MT requirements, the deficit part is supplied by the storage system. Otherwise, the surplus methane is stored in the storage tank. For the sake of safety, the amount of methane in the tank must be noticed and controlled.

When the stored methane in the tank reaches 90% of the tank volume, a signal is sent to the MPC system to decrease the input feed of the reactor. Otherwise, if the stored methane decreases to 30% of the tank volume, a signal is sent to the MPC to increase the input feed of the reactor. From an economic point of view, the presence of the storage tank makes the reactor more reliable and economic. Without a tank, the reactor cannot supply an electric load continuously in case of load increase. On the other hand, with load decrease, the produced methane may be greater than the load requirements and therefore it is necessary to the disposal of the surplus amount of methane to keep the pressure inside the reactor constant. This is not only an uneconomic decision but also an unsafe one.

III. Procedure for Solving Problem

This paper proposes an adaptive MPC system for the whole biogas power plant based on both MT parameters and the methane quantity stored in the tank. The computation procedure of the proposed control system is illustrated in Fig. 5 and can be summarized in the following steps.

Step 1: enter the input parameters of the state space and build MPC controller.

Step 2: feed the reactor with the specified animal manure (its biodegradable concentration must be identified).

Step 3: simulate the chemical reaction of the AD process to produce the appropriate amount of methane.

Step 4: according to the connected load, the methane required for supplying the load is passed to the MT, whereas the surplus methane is passed to the storage tank.

Step 5: in case of load change (increase or decrease), each MT and the tank sends signals to the MPC controller. The MT sends a speed signal according to load change. At the same time, the tank sends a signal dependent on its status (charged or discharged).

Step 6: if the load increases, the speed of MT decreases, and the MT speed controller sends a signal to MPC. If the amount of methane in the tank is at the permissible limits, the MPC sends a signal to the methane storage system to increase the output quantity for supplying the load requirements. Otherwise, if the load decreases, the MT speed increases. The MT speed controller sends a signal to MPC and the controller sends a signal to the storage system to decrease the methane.

Step 7: if the amount of methane in the tank reaches the prescribed maximum limit, the MPC controller sends a signal to the reactor to decrease the feed input. Otherwise, if the methane in the tank reaches the prescribed minimum limit of the tank, the MPC controller sends a signal to the reactor to increase the feed input.

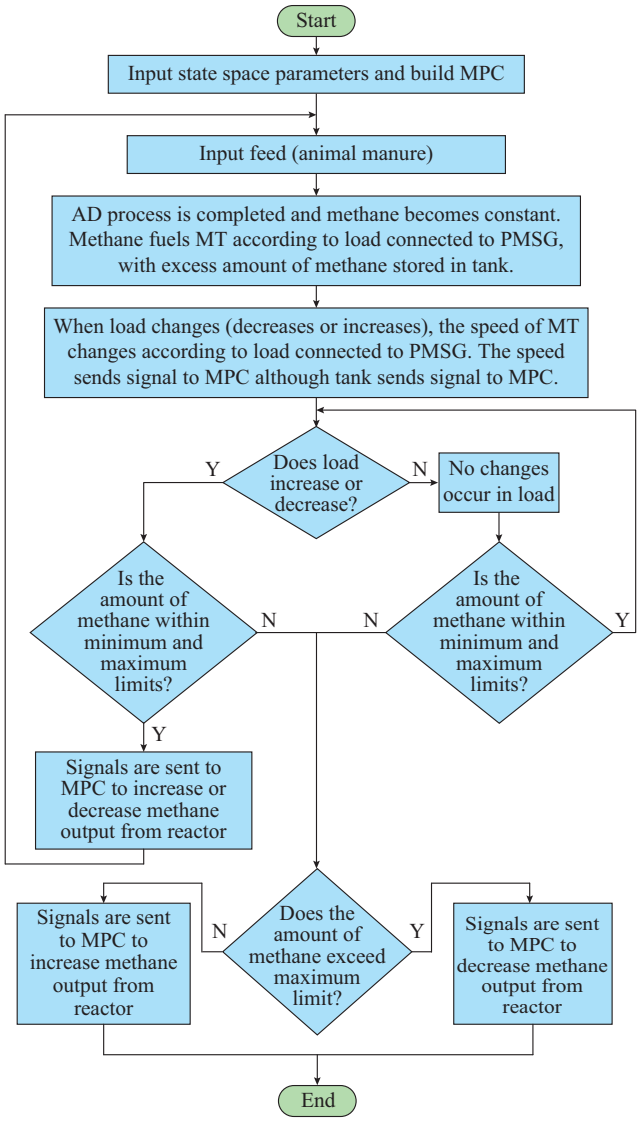

Fig. 5. Flowchart for proposed control system.

IV. Mathematical Modeling and Simulation

This section presents the mathematical modeling and simulation of the proposed control system. Reference [19] has proposed a complete Simulink model for a biogas-fueled power system, which is composed of three main parts: a biogas reactor, an MT coupled to a PMSG, and a storage system. This model will be used as a base model to simulate the proposed control system for a biogas power plant. In this section, a proposed adaptive control system is developed to optimally operate the biogas-fueled power system. The control system consists of three main parts, i.e., MT controllers, storage system controller, and biogas reactor controller. The MT controllers include speed controller, temperature controller, acceleration controller and fuel system controller. The following subsections describe the definition, function, and Simulink model of each controller. A complete Simulink model of the biogas power plant including all its control systems will be developed at the end of this section.

A. Speed Controller

Speed control is primary for the MT under partial load conditions. It operates on the speed error formed between a reference speed (one per unit) and the synchronous generator rotor speed. In this paper, the speed control is modeled using a lead-lag transfer function, or by a proportional integral derivative (PID) controller. The droop governor is the speed controller in which the output is proportional to the speed error [20]. The isochronous speed controller is a proportional-plus-reset speed controller, where the output change rate is proportional to the speed error. Any increase in the load leads to a decrease in speed and vice versa. Figure 6 represents a block diagram for this control function [20], [21]. In this figure, K is a controller gain; T_1, T_2 are the governor lead and lag time constants, respectively; and Z is a constant representing the governor mode.

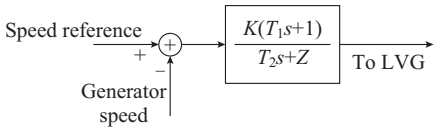

Fig. 6. Block diagram of MT speed controller.

B. Temperature Controller

Figure 7 illustrates a block diagram of the temperature controller. The temperature is transferred through the radiation shield to the thermocouple. The radiation shield (RS) and thermocouple (TC) transfer functions are represented by the following transfer functions [22]:

$$RS = 0.8 + \frac{2}{15(s+1)} \tag{4}$$

$$TC = \frac{1}{2.5(s+1)} \tag{5}$$

The turbine temperature T_X is compared to the desired reference value and controlled by a temperature PI controller with the transfer function [22]:

$$T_c = \frac{3.3(s+1)}{T_t s} \tag{6}$$

where T_t is the temperature controller integration (℃).

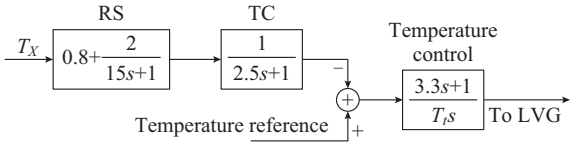

Fig. 7. Block diagram of temperature controller.

C. Acceleration Controller

Acceleration control is employed primarily during turbine startup to set the rate of the rotor acceleration prior to reaching the operating speed. Acceleration controller is an integrator as explained in Fig. 4. It acts on the error between the derivative of generator speed and the constant reference signal. If the operation speed of the system is close to its rated speed, the acceleration control can be eliminated in the modeling [20].

D. Fuel System Controller

The amount of the injected fuel to the MT is governed through a valve positioner (VP) controlled by a control signal V_{ce} resulted from the LVG. The fuel system consists of a fuel valve and an actuator. The fuel flows from the fuel system actuator through the VP. The VP is represented by the following transfer function [22]:

$$VP = \frac{a}{b(s+c)} \tag{7}$$

where a, b, c are the constants of the VP.

In this paper, the fuel system (FS) is presented by the following transfer function [22]:

$$FS = \frac{1}{T_F(s+1)} \tag{8}$$

where T_F is the fuel control time constant.

The function of the compressor in an MT is to supply a sufficient air quantity to satisfy the requirements of the combustion burners. The compressor increases the pressure of the air received from the air inlet duct, and then, discharges it to the burners at the required magnitude and suitable pressure. The fuel combustion (CB) process in the combustor is presented by the following transfer function [22]:

$$CB = \mathrm{e}^{-E_{CR}} \tag{9}$$

where E_{CR} is the combustion reaction time delay.

The transfer function representing the hot computation gas (CD) expansion is expressed as follow [22]:

$$CD = \frac{1}{T_{CD}(s+1)} \tag{10}$$

where T_{CD} is the discharge volume time constant.

Both the torque and exhaust temperature characteristics of a single-shaft gas turbine are essentially linear with respect to fuel flow and turbine speed. The produced mechanical torque T_M driving the electric generator is represented by the following equation [22]:

$$T_M = 1.3(CD - 0.23) = 0.5(1 - N) \tag{11}$$

where N is the rotor speed.

For MT temperature control, the turbine temperature T_X is computed by [22]:

$$T_X = T_R - 700\left(1 - \mathrm{e}^{-SE_{TD}}\right) + 550(1 - N) \tag{12}$$

where T_R is the reference temperature; and E_{TD} is the turbine exhaust delay.

The output of the LVG is the least amount of fuel needed for a specific operating point V_{ce} which will be the input to fuel system beside N. The per unit value of V_{ce} is directly proportional to that of the mechanical power on the turbine at steady state. Figure 8 shows a block diagram of the fuel flow control as a function of V_{ce}, where K_3 is the minimum amount of fuel flow without load.

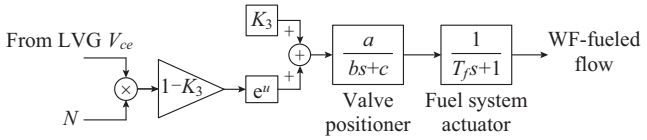

Fig. 8. Block diagram of fuel flow control system.

All the above controllers are represented in MATLAB/Simulink environment. The Simulink model for the MT including all proposed control systems is illustrated in [19].

E. Storage System Controller

The storage system consists of two parts. The first part is a comparator, which receives the signal coming from MT fuel controller for detecting the amount of methane needed by the MT and the amount of methane output from the reactor. The second part is the tank that stores the excess methane coming from the reactor. A Simulink model for the storage system is developed and illustrated in [19]. The required storage volume can be calculated by performing a mass balance over the storage volume as [23]:

$$V_{M,in} - V_{M,out} + \frac{\mathrm{d}V_{acc}}{\mathrm{d}t} = 0 \tag{13}$$

where $V_{M,in}$ and $V_{M,out}$ are the volumes of methane input to and output from the storage tank, respectively; and V_{acc} is the volume of methane accumulated in the storage tank.

The volume of methane storage in tank $V_{storage}$ is obtained by integration as:

$$V_{storage} = \int (V_{M,in} - V_{M,out})\mathrm{d}t \tag{14}$$

The biogas flow rate needed to supply the load connected to MT is calculated according to the following relation [20]:

$$V_{needed} = \frac{24P}{\eta_{MT} \cdot CV_{CH4} \cdot \omega_{CH4}} \tag{15}$$

where V_{needed} the volumetric flow rate of biogas needed; P is the output power of MT; η_{MT} is the efficiency of MT; CV_{CH4} is the calorific value of methane equal to 10 kWh/m^3; and ω_{CH4} is the percentage of methane in biogas, which is 70%-75%.

As explained before, in case that the stored methane in the tank exceeds the maximum prescribed limit of the tank volume, the control system will decrease the input feed to the reactor. Otherwise, if the stored methane decreases to less than the minimum prescribed limit of the tank volume, the control system will increase the input feed of the reactor.

F. Biogas Reactor Controller

There are many factors affecting the outputs of the reactor including the feed type, the reactor temperature, the moisture, the pH, etc. [24]. The main factor affecting the feed type is the concentration of biodegradable concentration [25]. There is a remarkable change in both methane production period and volume for different feed types.

In order to complete the fermentation process, the temperature of reactor T_{react} must be kept in a range between 20 ℃ and 60 ℃ [26]. If the reactor temperature exceeds 60 ℃, there will be a severe reduction in methanogenesis (bacteria) concentration. So, it is important to fix the temperature of the reactor at a set point, which is one of the tasks for the reactor controller.

1) Mathematical Modeling of Biogas Reactor

The mathematical model of the AD reactor operations depends on the material balances of volatile biodegradable solids, volatile fatty acids, acidogens and methanogens, and the computation of the flow of methane. In the literature, several mathematical models representing the dynamic behavior of AD reactors using animal wastes have been reported [27]-[29].

References [27] and [28] have presented a dynamic model of AD reactor based on Hill's model [29]. In this paper, the modified Hill's dynamic AD model is used as a mathematical model to represent the dynamic behavior of AD bioreactor feeding by dairy manure. The model can be summarized as:

$$\dot{S}_b = \left(B_o S_{vs} - S_b\right)\frac{F_{feed}}{V} - \frac{\mu_m S_b K_1 X_{acid}}{K_s + S_b} \tag{16}$$

$$\dot{S}_v = \left(A_f B_o S_{vs} - S_v\right)\frac{F_{feed}}{V} + \frac{\mu_m S_b K_2 X_{acid}}{K_s + S_b} - \frac{\mu_{mc} S_v K_3 X_{meth}}{K_{sc} + S_v} \tag{17}$$

$$\dot{X}_{acid} = \left(\frac{\mu_m S_b}{K_s + S_b} - K_d - \frac{F_{feed}}{bV}\right)X_{acid} \tag{18}$$

$$\dot{X}_{meth} = \left(\frac{\mu_{mc} S_v}{K_{sc} + S_v} - K_{dc} - \frac{F_{feed}}{bV}\right)X_{meth} \tag{19}$$

$$F_{meth} = V\frac{\mu_{mc} S_v}{K_{sc} + S_v}K_4 X_{meth} \tag{20}$$

$$\mu_m(T_{react}) = \mu_{mc}(T_{react}) = 0.013T_{react} - 0.129 \tag{21}$$

where S_b is the concentration of biodegradable volatile solid in the reactor; B_o is the biodegradability constant; S_{vs} is the concentration of volatile solid in influent; F_{feed} is the feed flow rate; V is the effective reactor volume; μ_m is the maximum reaction rate for acidogens; X_{acid} is the concentration of acidogens; K_1 is the yield factor estimated using experimental data given in [28]; K_s is the Monod half-velocity constant for acidogens; A_f is the acidity constant; X_{meth} is the concentration of methanogens; μ_{mc} is the maximum growth rate for

methanogens; S_v is the concentration of total volatile fatty acids in the reactor; K_2 is the yield factor estimated using experimental data; K_3 is the yield factor related to the growth rate of methane gas; K_{sc} is the Monod half-velocity constant for methanogens; b is the retention time factor estimated using experimental data [28]; K_d is the specific death rate of acidogens; K_{dc} is the specific death rate of a methanogens; K_4 is the factor related to the methane gas flow and estimated from experimental data [28]; and F_{meth} is the methane gas flow rate.

2) State Space and Model-based Control of Biogas Reactor

MPC uses a process model and the current state to predict future values of the output. Therefore, it is important for the MPC to detect the current state of the biogas plant so that the simulation can start successfully. The basis of the state space is the concentration of the resulting bacteria from each stage of the AD process. Hence, these concentrations are the state variables of the proposed model. The state variables of the model are the concentration of biodegradable volatile solid in the reactor S_b, the concentration of volatile solid in influent S_{vs}, the concentration of acidogens X_{acid}, and the concentration of methanogens X_{meth}.

The following equations are used to represent the state space of the proposed model:

$$\dot{\boldsymbol{X}} = \boldsymbol{A}\boldsymbol{X} + \boldsymbol{B}_1\boldsymbol{U} + \boldsymbol{B}_2\boldsymbol{W} \tag{22}$$

$$\boldsymbol{Y} = \boldsymbol{C}\boldsymbol{X} + \boldsymbol{D}_1\boldsymbol{U} + \boldsymbol{D}_2\boldsymbol{W} \tag{23}$$

$$\boldsymbol{X} = \begin{bmatrix} S_b \\ S_v \\ X_{acid} \\ X_{meth} \end{bmatrix} \tag{24}$$

$$\boldsymbol{A} = \begin{bmatrix} \frac{-F_{feed}}{V} & 0 & -\frac{\mu_m S_b K_1}{K_s + S_b} & 0 \\ 0 & \frac{-F_{feed}}{V} & \frac{\mu_m S_b K_2}{K_s + S_b} & -\frac{\mu_{mc} S_v K_3}{K_{sc} + S_v} \\ 0 & 0 & \frac{\mu_m S_b}{K_s + S_b} - K_d - \frac{F_{feed}}{bV} & 0 \\ 0 & 0 & 0 & \frac{\mu_{mc} S_v}{K_{sc} + S_v} - K_{dc} - \frac{F_{feed}}{bV} \end{bmatrix} \tag{25}$$

$$\boldsymbol{B}_1 = \begin{bmatrix} \frac{B_o S_{vs} - S_b}{V} \\ \frac{B_o A_f S_{vs} - S_v}{V} \\ -\frac{X_{acid}}{bV} \\ -\frac{X_{meth}}{bV} \end{bmatrix} \tag{26}$$

$$\boldsymbol{B}_2 = \begin{bmatrix} B_o \\ A_f B_o \\ 0 \\ 0 \end{bmatrix} \tag{27}$$

$$\boldsymbol{C} = \begin{bmatrix} 0 & 0 & 0 & V\frac{\mu_{mc} S_v}{K_{sc} + S_v} K_4 \end{bmatrix} \tag{28}$$

where $\boldsymbol{X}$ is a vector representing the state variables; $\boldsymbol{A}$ is a state or system matrix representing the factors of state variables; $\boldsymbol{U}$ is the input or control vector representing the input of the system, and $\boldsymbol{U} = \boldsymbol{F}_{feed}$; $\boldsymbol{B}_1$ is the input vector representing the factors of $\boldsymbol{F}_{feed}$ in each stage; $\boldsymbol{W}$ is the disturbance of the system, and $\boldsymbol{W} = \boldsymbol{S}_{vs}$; $\boldsymbol{B}_2$ is the vector representing the factors of disturbance in each stage; $\boldsymbol{Y}$ is the output vector representing the methane output from the AD process, and $\boldsymbol{Y} = \boldsymbol{F}_{meth}$; $\boldsymbol{C}$ is the output matrix representing the factors of $\boldsymbol{F}_{meth}$; and $\boldsymbol{D}_1$ and $\boldsymbol{D}_2$ are the feedthrough or feedforward matrices, respectively, and $\boldsymbol{D}_1 = \boldsymbol{D}_2 = \boldsymbol{0}$. If the system model does not have direct feedthrough, $\boldsymbol{D}_1$ and $\boldsymbol{D}_2$ are zero matrices.

A Simulink model for both the biogas power plant and the proposed MPC control system is developed. The model consists of all the prescribed submodels connected together. The biogas plant variables are controlled using the state space-MPC closed loop as explained in Fig. 2. The optimal substrate feed is achieved depending on the current state of the plant according to the MT speed and any load variations. To validate the performance of the proposed controller and prove its effectiveness and applicability, the system will be examined and analyzed under different operation conditions in the next section.

V. Simulation Results and Discussions

The proposed control system is simulated and tested under different loading conditions including variable and unbalanced loads. For the studied system, the fed substrate is the swine as it has a high concentration of biodegradable. The swine is diluted with 25% water and filtered with a sieve. The control variables of both MT and PMSG and the factors required for fully representing the AD process are obtained from experimental analysis given in [19]. The temperature of reactor is kept fixed at 35 ℃. The factors and parameters used in the proposed model are shown in Table AI in Appendix A.

It is well known that each cubic meter of biogas contains the equivalent of 6 kWh of heat energy. The same volume of biogas converted to electrical energy yields 1.3-1.8 kWh. The rest of the energy is dispersed as heat [28]. The amount of methane produced from the reactor is equal to 1.5-2.5 times the volume of the reactor [28]. The rated capacity of biogas plant is 400 kW, as the volume of the simulated reactor is taken as 160 m^3 [19]. The permissible limits of the storage tank are taken as 30%-90% of the tank volume.

The PC used in the simulation has an Intel(R) Core(TM) i3-2330M, with 2.20 GHz CPU and 2.00 GB of RAM.

A. Validation of Proposed Model

The proposed model is tested under a constant load to validate the applicability of the proposed MPC-based controller. The biogas plant is simulated with and without integrating the MPC to examine the performance of the biogas power plant when it feeds a constant load. The impact of the MPC-based controller on both MT torque and speed is firstly explored. Then, the impact on the methane produced by the re-

actor and that stored in the storage tank is discussed. In order to test the impact of the proposed controller on the storage system, the constant load is assumed as 100 kW which is less than the plant full load of 400 kW.

1) Impact on MT Torque and Speed

As explained before, the formation of methane in the reactor takes a few days to produce a constant amount of biogas. During this period, the MT torque increases with the produced methane until it reaches a constant value after completing the AD process.

Without applying a control system, the amount of input feed to the reactor is fixed at a daily step according to the designed size of the reactor. Since the nameplate capacity of the designed plant is 400 kW, any decrease in the connected load will not affect the input feed, leading to an increase in the surplus methane which may affect the system safety.

The aforementioned discussion presents the importance of utilizing an appropriate and efficient control system with biogas power plants. In the case of applying the proposed controller to the prescribed biogas power plant, there will be a reciprocal relationship between the load, the storage tank, and the input feed. In case the connected load decreases and the amount of methane stored in the tank exceeds the maximum permissible limit, the MPC controller sends a signal to the reactor to decrease the input feed.

Figure 9 explains the variation of MT torque and speed with and without MPC-based controller. Without applying MPC, the methane reaches a constant value after 20 days, and the torque increases with the volume of the produced methane. When the methane reaches a constant value of 300 m^3, the torque decreases to match the load, and the speed becomes constant. In the case of applying MPC, no transient occurs in the torque or speed due to the connection to the load.

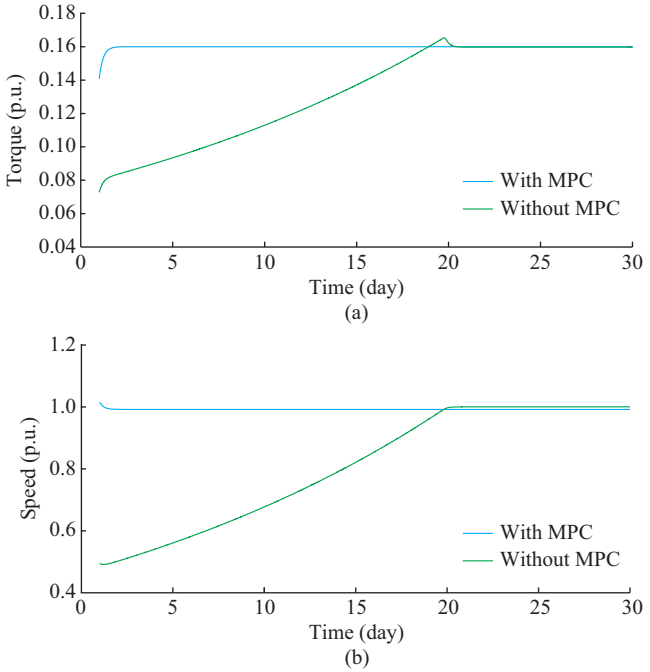

Fig. 9. Variation of MT torque and speed with and without MPC-based controller.

2) Impact on Methane Production

Without applying the MPC-based controller, the methane output from the reactor reaches 300 m^3 after 20 days. But in case of applying the proposed controller, the methane is changed (increase or decrease) according to the volume of the stored methane in both the storage tank and the connected load as shown in Fig. 10. Controlling the amount of produced methane is a great advantage of the proposed controller. In case the biogas plant is installed without a control system, a larger tank size is needed, which is shown by comparing the areas under the two curves in Fig. 10. The uncontrollable production of biogas may even lead to a tank explosion.

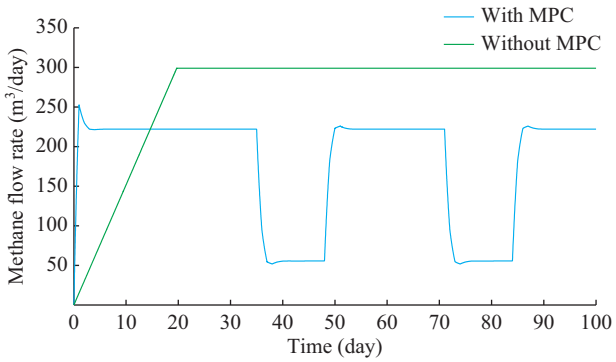

Fig. 10. Variation of produced Methane with constant load.

To examine the impact of the proposed controller on the storage system, the actual load connected to PMSG in this case is 100 kW, whereas the full load of the plant is 400 kW. Figure 11 shows the volume of methane stored in the tank without applying MPC controller to the plant. In this case, there is a daily increase in the methane stored in the tank. The stored methane exceeds the size of the designed tank on the 54th day. The size of the tank must be increased or there will be a risk of tank explosion.

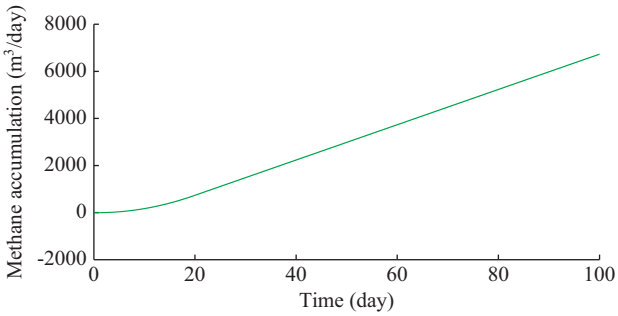

Fig. 11. Variation of accumulated methane with constant load without MPC.

By applying the proposed controller, there will be different actions in the biogas plant. Whenever the methane in the tank reaches 90% (1800 m^3) of the tank volume (2000 m^3), the controller sends a signal to the reactor to decrease the input feed, and hence, to decrease the produced methane. This action is done on the 32nd day and the 72nd day. In case that the methane stored in the tank reaches 30% (600 m^3) of the

tank volume, the controller sends a signal to the reactor to increase the input feed, and hence, to increase the produced methane. This action is done on the 45th day and the 88th day as shown in Fig. 12.

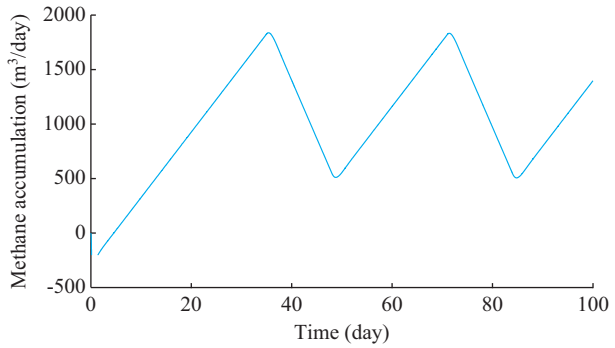

Fig. 12. Variation of accumulated methane with constant load with MPC.

The next two sub-sections will analyze the impact of load variations on the controller's performance for balanced and unbalanced loads.

B. Normal Operation

In this sub-section, a hypothetical load curve is used to study the behaviors of the proposed control system due to load variations over a specified period. The load curve is shown in Fig. 13.

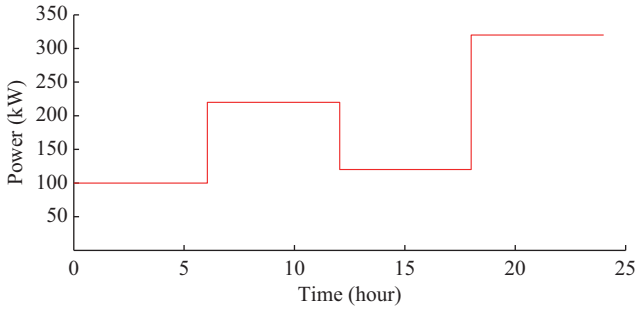

Fig. 13. Studied load curve.

The performances of MT, reactor, and storage system are studied and analyzed during load changes. The examined performances include the impacts of load variations on methane production in the presence of the proposed MPC controller.

The impact of load change on the generator speed is shown in Fig. 14. Without applying the MPC, the speed decreases whenever the load increases (at the 28th and 40th hours). On the other hand, the generator speed increases whenever the load decrease (at the 34th hour). In the case of applying the MPC, the speed becomes nearly constant during load change, and the speed variations are within [−5%, + 7%].

Figure 15 shows the variation of the produced methane with load before applying the proposed controller. In the case of applying the controller, the methane output from the reactor is affected by the load connected to MT and the amount of methane stored in the tank. If the load increases as in the case of the 28th hour and the 40th hour, the methane produced in the reactor increases at the 28th hour due to the increasing feed input to the reactor. Whenever the methane stored in the tank reaches 90% of the tank volume at the 31st hour, the controller sends a signal to the reactor to decrease the feed input so that the produced methane decreases. The variation of the produced methane stored in the tank for this case is shown in Fig. 16.

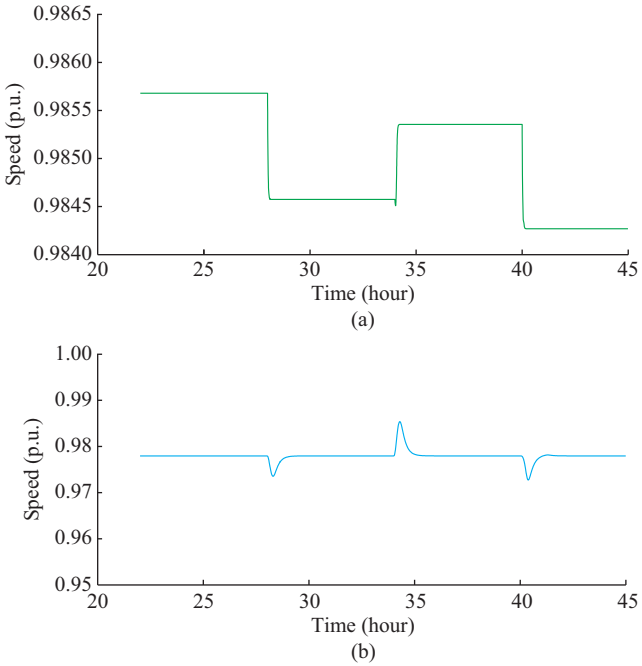

Fig. 14. Variation of generator speed with load. (a) Without MPC. (b) With MPC.

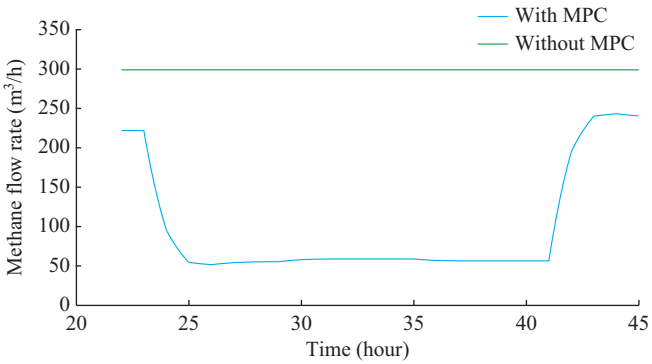

Fig. 15. Variation of produced methane with load.

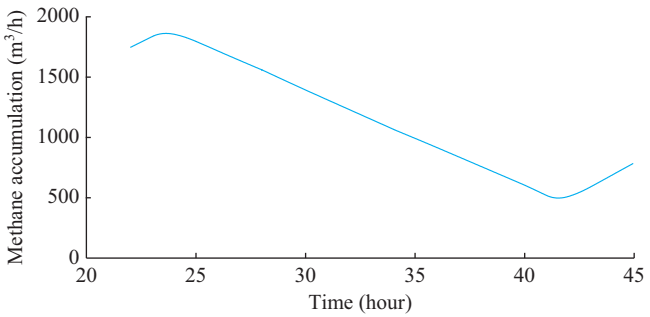

Fig. 16. Variation of accumulated methane in tank with MPC controller.

Figure 17 shows the methane needed by the load, the methane produced by the reactor and the methane stored in the tank. The summation of the amount of methane required by the load and the amount of methane stored in tank equal to the amount of methane produced from the reactor as shown by the figure.

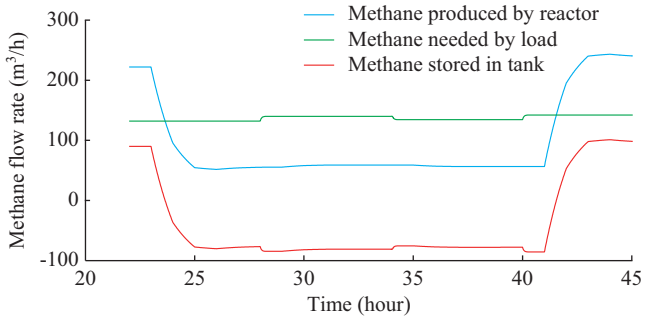

Fig. 17. Variation of methane with variable load when applying MPC controller.

C. Unbalanced Load Operation

To explore the effectiveness of the proposed controller, the MPC controller is examined under unbalanced loading condition. The unbalanced load occurs at the PMSG terminals for 6 s (from $t=30$ s to $t=36$ s). The performances of MT and generator are studied during this period. The studied performance includes the impact of unbalanced load on MT torque, generator speed, and generator output voltage.

1) Impact on MT Torque

Without applying any controller, a high mechanical vibration occurs in the MT shaft during the unbalanced loading condition as shown in Fig. 18(a). These high vibrations put the MT at the risk of breaking-down. In the case of applying the proposed MPC-based controller, these vibrations are highly decreased as shown in Fig. 18(b). By applying the MPC performance index, it is explained that the error is decreased from 18% to 2% using the proposed controller. The control system succeeds in decreasing the variation as its functions are based on measuring the currents and predicting the future values of the outputs. In addition, the objective of the MPC method is to determine the sequence of control movements so that the expected response moves to the set point in an optimal manner.

2) Impact on Generator Speed

Without applying MPC, high disturbance occurs on the speed of the generator due to the high mechanical stresses on the MT shaft as illustrated by Fig. 19(a). In the case of applying the proposed MPC, these disturbances are decreased and the speed reaches the nominal value as shown in Fig. 19(b). By applying the MPC performance index, it is explained that the error is decreased from 50% to 10% using the proposed controller.

3) Impact on Generator Output Voltage

For the base case without applying the controller, the output voltage oscillates by higher values due to the MT mechanical vibrations. In the case of applying the proposed controller, the oscillations are decreased and the output voltage becomes a pure sinusoidal wave. By measuring the performance index, the error is decreased from 15% to 0%. Figure 20 shows the impact of unbalanced load operation on the generator output voltage.

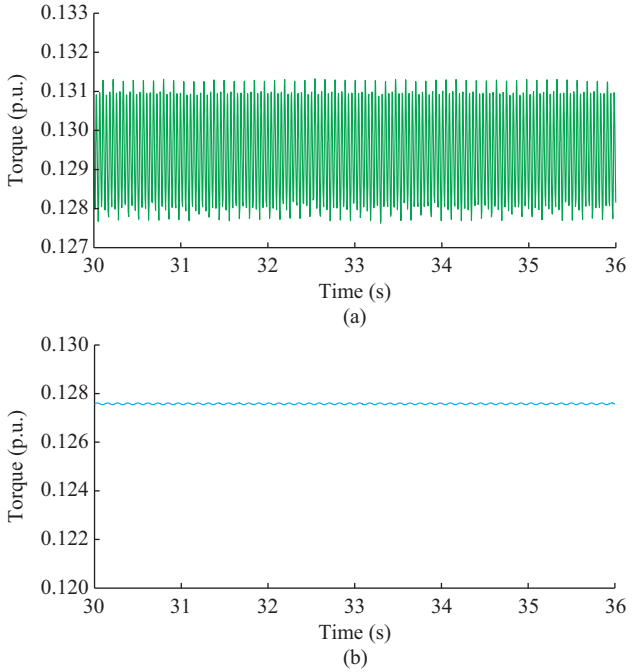

Fig. 18. Variation of MT torque with unbalanced load condition. (a) Without MPC. (b) With MPCE.

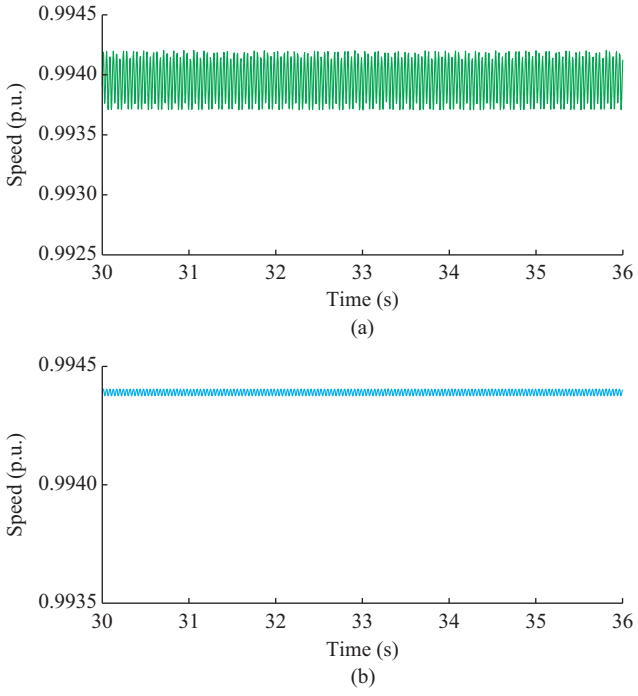

Fig. 19. Variation of generator speed with unbalanced load condition. (a) Without MPC. (b) With MPC.

The computation complexity of the proposed model is related to the number of resources required for running it. The resource that is most commonly considered is the time com-

plexity. The usual units of time are not used in complexity theory, because they are too dependent on the choice of a specific computer or the evolution of technology. Therefore, instead of the real time, one generally considers the elementary operations that are done during the computation. The excution time of the simulation model ranges from 12 s to 15 s.

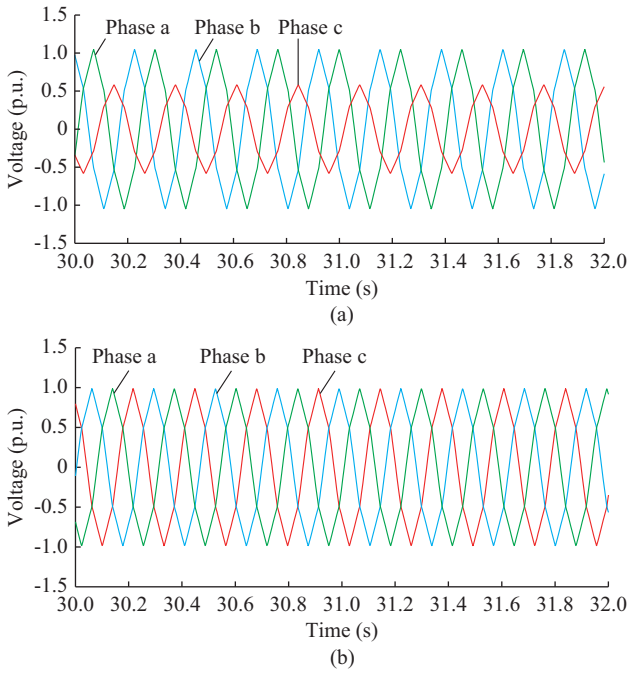

Fig. 20. Variation of generator output voltage with unbalanced load condition. (a) Without MPC. (b) With MPC.

VI. Conclusion

This paper has presented an adaptive control system using MPC for a biogas power plant based on state space. The proposed control system has been developed to control the fed substrate according to the connected load, and respond to the expected changes in the electric load.

The control scheme is derived from an anaerobic digestion model, which includes all the concentrations of biodegradable volatile solid in the reactor, volatile solid in influent, acidogens, and methanogens. Those are the state variables of an MPC system.

The system has been implemented in the MATLAB/Simulink environment and tested under different loading conditions. The simulation results have proved the effectiveness and applicability of the proposed MPC system to adapt the biogas power plant operation under different operating conditions. The proposed controller system can protect the MT from the damage due to unbalanced load operation by decreasing the duration and values of the disturbances. By measuring the performance index, the errors decrease from 18% to 2% for the MT torque, from 50% to 10% for the generator speed, and from 15% to 0% for the generator output voltage, respectively.

Appendix A

TABLE AI
Factors and Parameters Used in Proposed Model

Item	Parameter	Value
AD	B	2.90
	K_s	15.5 kg/m^3
	K_{sc}	3 kg/m^3
	K_d	0.02 day^{-1}
	K_{dc}	0.02 day^{-1}
	K_1	3.89
	K_2	1.76
	K_3	31.7
	K_4	26.3
	A_f	0.69
	B_o	0.25
	V	160 m^3
MT	A	1
	B	0.05
	C	1
	T_1	0.4
	T_2	1
	K	25
	T_F	0.04
	t_R	510 ℃
	T_t	232.2 ℃
	Z	3
	E_{CR}	0.01
	E_{TD}	0.04
	T_{CD}	0.2
PMSG	R	12.5 Ω
	L_d	165 μH
	L_q	165 μH
	W_r	70000 r/min
	P	4 poles
	J	0.011 kg·m^2
	λ	0.2388 Wb

References

[1] K. Singh and T. Jash, "Performance analysis of microturbine-based grid-connected biogas power plant in Purulia in West Bengal, India," *Clean Technologies and Environmental Policy*, vol. 17, no. 3, pp. 789-795, Aug. 2015.

[2] J. Bailey and D. Ollis, *Biochemical Engineering Fundamentals*, 2nd ed. New York: McGraw-Hill, 1984.

[3] D. Nguyen, V. Gadhamshetty, S. Nitayavardhana *et al.*, "Automatic process control in anaerobic digestion technology: a critical review," *Bioresource Technology*, vol. 193, pp. 513-522, Oct. 2015.

[4] F. Haugen, R. Bakke, and B. Lie, "Temperature control of a pilot anaerobic digestion reactor," *Modeling, Identification and Control*, vol. 33, no. 4, pp. 99-117, Jul. 2013.

[5] F. Haugen, R. Bakke, and B. Lie, "On-off and PI control of methane gas production of a pilot anaerobic digestion reactor," *Modeling, Identification and Control*, vol. 34, no. 3, pp. 139-156, Jul. 2013.

[6] A. Rincón, C. Erazo, and F. Angulo, "A robust adaptive controller for an anaerobic digester with saturated input: guarantees for the boundedness and convergence properties," *Journal of Process Control*, vol. 22, no. 9, pp. 1785-1792, Oct. 2012.

[7] L. Xue, D. Li, and Y. Xi, "Nonlinear model predictive control of an-

aerobic digestion process based on reduced ADM1," in *Proceedings of 10th Asian Control Conference (ASCC)*, Kota Kinabalu, Malaysia, Sept. 2015, pp. 1-6.
[8] D. Gaida, C. Wolf, T. Bäck *et al*., "Nonlinear model predictive substrate feed control of biogas plants," in *Proceedings of 20th Mediterranean Conference on Control & Automation*, Barcelona, Spain, Aug. 2012, pp. 1-6.
[9] D. Gaida, A. L. S. Brito, C. Wolf *et al.*, "Optimal control of biogas plants using nonlinear model predictive control," in *Proceedings of 22nd IET Irish Signals and Systems Conference*, Dublin, Ireland, Jun. 2011, pp. 1-6.
[10] O. Bernard, M. Polit, Z. Hadj-Sadok *et al.*, "Advanced monitoring and control of anaerobic wastewater treatment plants: software sensors and controllers for an anaerobic digester," *Water Science and Technology*, vol. 43, no. 7, pp. 175-182, Sept. 2001.
[11] G. Oppong, G. Montague, B. Elaine *et al*., "Towards model predictive control on anaerobic digestion process," *IFAC Proceedings Volumes*, vol. 46, no. 32, pp. 684-689, Dec. 2013.
[12] A. Ordace, C. M. Ionescu, T. P. W. Vannecke *et al.*, "Predictive control of anaerobic digestion of wastewater sludge: a feasibility study," in *Proceedings of 16th International Conference on System Theory, Control and Computing*, Sinaia, Romania, Dec. 2012, pp. 1-7.
[13] C. García-Diéguez, F. Molina, and E. Roca, "Multi-objective cascade controller for an anaerobic digester," *Process Biochemistry*, vol. 46, no. 4, pp. 900-909, Apr. 2011.
[14] D. Gaida, C. Wolf, and M. Bongards, "Feed control of anaerobic digestion processes for renewable energy production: a review," *Renewable and Sustainable Energy Reviews*, vol. 68, no. 2, pp. 869-875, Feb. 2017.
[15] P. Orukpe, "Model predictive control fundamentals," *Nigerian Journal of Technology*, vol. 31, no. 2, pp. 139-148, Jul. 2012.
[16] M. O'Brien, J. Mack, B. Lennox *et al.*, "Model predictive control of an activated sludge process: a case study," *Control Engineering Practice*, vol. 19, no. 1, pp. 54-61, Jan. 2011.
[17] F. Camacho and C. Bordons, *Model Predictive Control*, 2nd ed. London: Springer Verlag, 2007.
[18] J. Rossiter, *Model-based Predictive Control: a Practical Approach*. Boca Raton: CRC Press, 2003.
[19] M. Saeed, S. Fawzy, and M. El-Saadawi, "Modeling and simulation of biogas-fueled power system," *International Journal of Green Energy*, vol. 16, no. 2, pp. 125-151, Jul. 2019.
[20] S. Guda, "Modeling and power management of a hybrid wind microturbine power generation system," M.Sc. Dissertation, Electrical Engineering Department, Montana State University, Bozeman, USA, 2005.
[21] S. Guda, C. Wang, and M. Nehrir, "Modeling of microturbine power generation systems," *Electric Power Components and Systems*, vol. 34, no. 9, pp. 1027-1041, Sept. 2006.
[22] W. Rowen, "Simplified mathematical representations of heavy-duty gas turbines," *Journal of Engineering for Power*, vol. 105, no. 4, pp. 865-869, Oct. 1983.
[23] R. Al-Zubi, "Modeling and performance analysis of a hybrid biogas-photovoltaic system," M. Sc. Dissertation, Electrical Engineering Department, Cairo University, Cairo, Egypt, and Faculty of Electrical Engineering and Computer Science, Kassel University, Kassel, Germany, 2012.
[24] A. Khalid, M. Arshad, M. Anjum *et al.*, "The anaerobic digestion of solid organic waste," *Waste Management*, vol. 31, no. 8, pp. 1737-1744, Aug. 2011.
[25] A. Husain, "Mathematical models of the kinetics of anaerobic digestion–a selected review," *Biomass and Bioenergy*, vol. 14, no. 5-6, pp. 561-571, May-Jun. 1998.
[26] T. Pathmasiri, F. Haugen, and S. Gunawardena, "Simulation of a biogas reactor for dairy manure," *Annual Transactions of IESL*, vol. 2013, pp. 394-398, Sept. 2013.
[27] F. Haugen, R. Bakke, and B. Lie, "State estimation and model-based control of a pilot anaerobic digestion reactor," *Journal of Control Science and Engineering*, vol. 2014, no. 3, pp. 1-19, Apr. 2014.
[28] H. Finn, R. Bakke, and B. Lie, "Mathematical modelling for planning optimal operation of a biogas reactor for dairy manure," in *Proceedings of World Congress on Water, Climate and Energy*, Dublin, Ireland, May 2012, pp. 1-9.
[29] D. Hill, "Simplified Monod kinetics of methane fermentation of animal wastes," *Agricultural Wastes*, vol. 5, no. 1, pp. 1-16, Jan. 1983.

Samaa Fawzy received the B.Sc. degree from Mansoura University, Mansoura, Egypt, in 2015, and the M.Sc. degree in electrical power and machines engineering from Mansoura University in 2019. She has been a researcher at the Electrical Engineering Department, Faculty of Engineering, Mansoura University since 2015. Her research interests include renewable energy, biomass energy, and adaptive control systems.

Mohammed Saeed received the B.Sc., M.Sc. and Ph.D. degrees from Mansoura University, Mansoura, Egypt, in 2004, 2010 and 2015, respectively. Currently, he is an assistant professor at the Electrical Engineering Department, Faculty of Engineering, Mansoura University. His research interests include renewable energy, biomass energy, smart grids, advanced control, modern optimization techniques, and power system analysis.

Abdelfattah Eladl received the B.Sc., M.Sc., and Ph.D. degrees from the Electrical Engineering Department, Faculty of Engineering, Mansoura University, Mansoura, Egypt, in 2002, 2007, and 2015, respectively. In 2016, he receives the best Ph.D. thesis award from Mansoura University. Currently, he is an assistant professor at the Electrical Engineering Department, Mansoura University. His research interests include power system economics, planning, power quality, and energy hubs.

Magdi El-Saadawi received the B.Sc. and M.Sc. degrees from Mansoura University, Mansoura, Egypt, in 1982 and 1988, respectively, and his Ph.D. from Warsaw University of Technology, Warsaw, Poland, in 1997. He was a teaching assistant at El-Mansoura University, Mansoura, Egypt, from 1983 to 1992. From 1997, he was a staff member of the Electrical Engineering Department, Mansoura University, and has been a professor since May 2011. His research interests include renewable energy, power system analysis, and applications of artificial intelligence in power systems.